Exclusive ρ and J/Ψ photoproduction in ultraperipheral pO and OO collisions at energies available at the CERN Large Hadron Collider

Victor P. Gonçalves [*]

Institut für Theoretische Physik, Westfälische Wilhelms-Universität Münster, Wilhelm-Klemm-Straße 9, D-48149 Münster, Germany;
Institute of Modern Physics, Chinese Academy of Sciences, Lanzhou 730000, China;
and Institute of Physics and Mathematics, Federal University of Pelotas, Postal Code 354, 96010-900 Pelotas, Rio Grande do Sul, Brazil

Bruno D. Moreira[†] and Luana Santana [‡]

Departamento de Física, Universidade do Estado de Santa Catarina, 89219-710 Joinville, Santa Catarina, Brazil

Collisions with oxygen ions at the CERN Large Hadron Collider (LHC) opens the possibility of investigating the description of the QCD dynamics in an unexplored regime, complementary to those performed in pp, pPb, and PbPb collisions. In this paper we estimate the exclusive ρ and J/Ψ photoproduction in ultraperipheral pO and OO collisions at the LHC using the color dipole formalism and considering distinct models for the dipole-target scattering amplitude and different approaches for the modeling of the vector meson wave function. We present our predictions for the rapidity and transverse momentum distributions, as well as for the total cross sections considering the rapidity ranges covered by the ALICE and LHCb detectors. Such results indicate that a future experimental analysis of these final states is feasible and that its study can be useful to improve our understanding of the QCD dynamics at high energies.

I. INTRODUCTION

The CERN Large Hadron Collider (LHC) recently started its Run 3 with the great expectation of new and more precise experimental data that will improve our understanding of the standard model and allow us to search for new physics in not yet explored kinematical regions. For this new run, the LHC physics programme provides data-taking campaigns with various colliding systems with distinct center-of-mass energies and characterized by different integrated luminosities [1]. In particular, proton-oxygen (pO) and oxygen-oxygen (OO) collisions are expected to be studied in the forthcoming years, which will achieve large integrated luminosities in modest running times [2]. As summarized in Ref. [3], these collisions will provide unique opportunities, due to the fact that they will allow us to investigate in detail the transition regime of several phenomena that are expected to have different behaviors in lead-lead (PbPb) and and proton-proton (pp) collisions [4] and they will also provide valuable data for cosmic-ray

---
[*]barros@ufpel.edu.br
[†]bduartesm@gmail.com
[‡]luana.s@edu.udesc.br

modeling [5]. Moreover, the study of pO collisions will also provide important constraints in the nuclear dependence of the parton distribution functions and in the small-x physics (see, e.g., Ref. [6]).

In this paper we investigate the exclusive vector meson photoproduction in ultraperipheral pO and OO collisions as a probe of the QCD dynamics at high energies. In these collisions the impact parameter is larger than the sum of the radii of the incident particles, making the photon-induced processes be dominant [7]. Our goal is to complement the previous studies performed for pp, pPb, PbPb, and XeXe collisions and present the predictions for the rapidity and transverse momentum distributions, derived considering distinct approaches for the description of the dipole-target interaction and for the treatment of the vector meson wave function (see, e.g., Refs. [8–10]). Our study is strongly motivated by the fact that the saturation scale Q_s, which characterizes the transition line between the linear and nonlinear regimes of the QCD dynamics [11], is predicted to be energy dependent and atomic number dependent. As a consequence, oxygen collisions provide the opportunity to probe the saturation effects in a new kinematical regime. In what follows, we focus on the ρ and J/Ψ photoproduction which, as demonstrated in Ref. [8], map different configurations of the dipole size and probe distinct regimes of the QCD dynamics. We present predictions for pO collisions at $\sqrt{s} = 9$ TeV and OO collisions at $\sqrt{s} = 5.52$ TeV, which are possible values for the future runs, but results for other configurations can be provided under request. It is important to emphasize that distinctly from the J/Ψ photoproduction, where the J/Ψ mass provides the hard scale
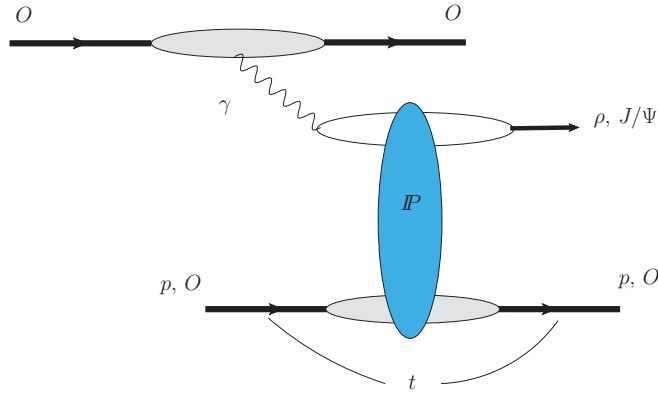
FIG. 1. Exclusive vector meson photoproduction in ultraperipheral pO and OO collisions.

that justifies the perturbative calculation, the analysis of the ρ photoproduction using the dipole approach is a theme of debate in the literature. For low energies, $Q^2 \approx 0$, and small values of squared momentum transfer t, the ρ photoproduction is dominated by large dipoles, where nonperturbative contributions become non-negligible. However, if nonlinear effects are taken into account, another scale is present in the process: the saturation scale Q_s, which increases with the energy and with the atomic mass number. The possibility that Q_s provides the hard scale to justify the calculation of the ρ photoproduction has been considered in the literature [9,10,12–16], with the predictions in reasonable agreement with the HERA and ALICE data. Motivated by these previous studies and by the possibility of testing this strong assumption in future runs of the LHC, we present here the dipole predictions for the ρ photoproduction in pO and OO collisions.

This paper is organized as follows. In the next section we present a brief review of the color dipole formalism for the exclusive vector meson photoproduction and the models used as input in our calculations are discussed. Our predictions for the vector meson photoproduction in pO and OO collisions are presented in Sec. III and the main conclusions are summarized in Sec. IV.

II. FORMALISM

Over the last two decades, the study of the vector meson photoproduction in hadronic colliders, proposed originally in Refs. [17–19], became a reality and it is currently considered the most promising process to improve our understanding of the QCD dynamics and to probe the the transverse spatial distributions of gluons in the target [20]. As the description of this process using the dipole formalism has been largely discussed in the literature (see, e.g., Refs. [7,20]), in what follows we only present a brief review of the main formulas needed for the calculation of the observables presented in this paper. The exclusive vector meson photoproduction in pO and OO collisions is represented in Fig. 1, and the associated differential cross section, for a given center-of-mass energy

$\sqrt{s}$, can be expressed as follows:[1]

$$\frac{d\sigma[h_1 + h_2 \rightarrow h_1 \otimes V \otimes h_2]}{dY\,dt}$$
$$= \left[n_{h_1}(\omega) \frac{d\sigma}{dt}(\gamma h_2 \rightarrow V \otimes h_2) \right]_{\omega_L}$$
$$+ \left[n_{h_2}(\omega) \frac{d\sigma}{dt}(\gamma h_1 \rightarrow V \otimes h_1) \right]_{\omega_R}, \qquad (1)$$

where $h_i = p$ or O, and the rapidity (Y) of the vector meson in the final state is determined by the photon energy ω in the collider frame and by the mass M_V of the vector meson [$Y \propto \ln(\omega/M_V)$]. Moreover, $d\sigma/dt$ is the differential cross section for the $\gamma h_i \rightarrow V \otimes h_i$ process, with the symbol $\otimes$ representing the presence of a rapidity gap in the final state and $\omega_L\ (\propto e^{-Y})$ and $\omega_R\ (\propto e^Y)$ denoting the energies of the photons emitted by the hadrons h_1 and h_2, respectively. Furthermore, $n_{h_i}(\omega)$ denotes the equivalent photon spectrum of the relativistic incident hadron, with the flux of a nucleus being enhanced by a factor Z^2 in comparison to the proton one. As in Refs. [8–10], we assume that the photon flux associated with the proton and with the nucleus can be described by the Drees-Zeppenfeld model [22] and the relativistic pointlike charge model [7], respectively. In the dipole picture one has that $d\sigma/dt$ is given by

$$\frac{d\sigma}{dt} = \frac{1}{16\pi} \left| \mathcal{A}_T^{\gamma h \rightarrow Vh}(x, \Delta) \right|^2, \qquad (2)$$

with the scattering amplitude being given by

$$\mathcal{A}_T^{\gamma h \rightarrow Vh}(x, \Delta) = i \int dz\,d^2\mathbf{r}\,d^2\mathbf{b}_h e^{-i[\mathbf{b}_h - (1-2z)\mathbf{r}/2]\cdot\mathbf{\Delta}}\,(\Psi^{V*}\Psi)_T$$
$$\times 2\mathcal{N}_h(x, \mathbf{r}, \mathbf{b}_h), \qquad (3)$$

where Δ denotes the transverse momentum lost by the outgoing hadron ($t = -\Delta^2$) and $\mathbf{b}_h$ is the position of the center of the $q\bar{q}$ dipole. Moreover, $(\Psi^{V*}\Psi)_T$ denotes the overlap of the transverse photon and vector meson wave functions and $z\,(1-z)$ is the longitudinal momentum fractions of the quark (antiquark). For a detailed discussion about the phase factor, see, e.g., Refs. [23,24]. As in previous studies [8,10], we consider the Gauss light cone (GLC) and boosted-Gauss (BG) models for the overlap function in order to estimate the impact of the modeling of the vector meson wave function on our predictions. Both models assume that the vector meson is predominantly a quark-antiquark state and that the spin and the polarization structure are the same as those in the photon [25–28], but differ on the description of the scalar part of the wave function (for a more detailed discussion, see, e.g., Ref. [8]).

One has that the differential cross section for hadronic collisions, Eq. (1), is proportional to the square of $\mathcal{N}_h(x, \mathbf{r}, \mathbf{b}_h)$, which is the nonforward scattering amplitude of a dipole of size $\mathbf{r}$ on the hadron target for a given value of $x = M_V^2/W^2$,

---

[1] For a recent discussion about the impact of the quantum mechanical interference between these two processes at the amplitude level, see, e.g., Ref. [21].

where the γh center-of-mass reaction energy is given by $W = [2\omega\sqrt{s}]^{1/2}$. Such strong dependence implies that the exclusive vector meson photoproduction in ultraperipheral collisions is sensitive to the description of the QCD dynamics at high energies [12], which determines $\mathcal{N}_h$. Moreover, the analysis of the t dependence of the predictions can be used to constrain the impact-parameter dependence of $\mathcal{N}_h$, since $\sqrt{-t}$ and $\boldsymbol{b}_h$ are Fourier-conjugated variables. It is important to emphasize that recent results indicate that the Fourier transform of $d\sigma/dt$ for exclusive processes can be used to obtain the transverse spatial distributions of gluons in the target and probe the gluon generalized parton distribution (see, e.g., Refs. [23,24]). Following Refs. [8–10], we assume, for a proton target, the phenomenological models proposed in Refs. [28,29] that successfully describe the ep HERA data for inclusive and exclusive processes [29,30]. It will allow us to estimate the current theoretical uncertainties associated with the QCD dynamics in the predictions for the exclusive vector meson photoproduction. The bCGC and IP-Sat models are based on distinct approximations of the color glass condensate (CGC) formalism [31] but predict different behaviors for the linear regime and for transition between the linear and nonlinear regimes. One has that the bCGC model interpolates two analytical solutions of well-known evolution equations: the solution of the Balitsky-Fadin-Kuraev-Lipatov (BFKL) equation near the saturation regime and the solution of the Balitsky-Kovchegov equation deeply inside the saturation regime. The underlying assumption is that the interaction between gluonic ladders is taken into account by the bCGC model, with the saturation boundary being approached via the BFKL equation. Moreover, this model assumes that the saturation scale depends on the impact parameter (IP-Sat model). The free parameters were fixed by fitting the HERA data and here we use the updated parameters obtained in Ref. [32]. On the other hand, the IP-Sat model [30] assumes an eikonalized form for $\mathcal{N}_p$ that depends on a gluon distribution evolved via the Dokshitzer-Gribov-Lipatov-Altarelli-Parisi (DGLAP) equation. This model resumes higher twist contributions and, distinctly from the bCGC model, the linear regime is described by the DGLAP evolution [33]. In this work, we employ the parameters obtained in Ref. [30]. Finally, for a nuclear target ($A = 16$), we estimate $\mathcal{N}_\mathrm{O}$ assuming the Glauber-Gribov formalism [34–37], which predicts that[2]

$$\mathcal{N}_\mathrm{O}(x, \boldsymbol{r}, \boldsymbol{b}_\mathrm{O}) = 1 - \exp\left[-\tfrac{1}{2}\sigma_{dp}(x, \boldsymbol{r}^2) T_\mathrm{O}(\boldsymbol{b}_\mathrm{O})\right], \quad (4)$$

where the nuclear profile function for the oxygen, $T_\mathrm{O}(\boldsymbol{b}_\mathrm{O})$, is described by a Woods-Saxon distribution, and $\boldsymbol{b}_\mathrm{O}$ is the transverse distance from the center of the ion to the center of mass of the $q\bar{q}$ dipole. The dipole-proton cross section σ_{dp}

is given by

$$\sigma_{dp}(x, \boldsymbol{r}^2) = 2 \int d^2\boldsymbol{b}_p \, \mathcal{N}_p(x, \boldsymbol{r}, \boldsymbol{b}_p). \quad (5)$$

In our analysis, the bCGC and IP-Sat models for a proton target are used as input to estimate $\mathcal{N}_\mathrm{O}(x, \boldsymbol{r}, \boldsymbol{b}_\mathrm{O})$.

Two comments are in order. In recent years, several authors have studied the impact of subnucleonic fluctuations on the description of exclusive processes (for a recent review, see Ref. [39]) and obtained that the t distribution for the incoherent vector meson photoproduction is sensitive to these event-by-event fluctuations of the spatial gluon distribution in the target (see, e.g., Refs. [21,24,40–43]). In contrast, for the coherent production, the impact of the geometry evolution on the rapidity and transverse momentum distributions is small, with the predictions with and without fluctuations being almost identical. As our focus in this paper is in the coherent vector meson photoproduction, we neglect the geometric evolution of the target in what follows. Another important comment is that, over the last years, several groups have improved the treatment of exclusive processes in the dipole approach, by estimating higher-order corrections for the evolution of the forward dipole-target scattering amplitude and the photon impact factor, as well as by improving the description of the vector meson wave function (see, e.g., Refs. [44–49]). Such results indicate that the NLO corrections are numerically important, but their effect can be partially captured when the initial condition for the small-x evolution of the dipole amplitude is fitted to the structure function data. Moreover, the next-leading-order (NLO) predictions for the vector meson photoproduction at HERA are similar to those obtained using the phenomenological dipole models, in particular to those derived using the bCGC model considered in this paper. Therefore, in principle, we do not expect a large modification of our predictions if the NLO corrections are taken into account. Surely, a more detailed comparison between our results and those derived at the NLO is an important next step, which we plan to perform in a future study.

III. RESULTS

Initially, let us discuss the main ingredients of our calculations: the dipole-proton scattering amplitude $\mathcal{N}_p$ and the overlap function $(\Psi^{V*}\Psi)_T$. In Fig. 2 we present $\mathcal{N}_p$ as a function of the dipole size r for two distinct values of x and central collisions ($b_p = 0$). considering the bCGC and IP-SAT models. For comparison, we also present the predictions of the IP-NONSAT model, which is the linear limit of the IP-SAT model, i.e., such a model disregards the contributions of the nonlinear corrections for the QCD dynamics. We have that the description of the linear regime (small-r) is distinct in the bCGC and IP-SAT models, as well the transition between the linear and nonlinear regimes, with the onset of the saturation regime ($\mathcal{N}^p \approx 1$) being slower in the case of the bCGC model. For small dipole sizes and $x = 10^{-3}$, we can observe the different r dependencies of the distinct models. In this regime, the bCGC model predicts that $\mathcal{N}^p \propto r^{2\gamma_\mathrm{eff}}$ for $r^2 \to 0$, with $\gamma_\mathrm{eff} \leqslant 1.0$, while the IP-SAT and IP-NONSAT models predict

---

[2]It is important to emphasize that the Glauber-Mueller formalism implies that the dipole-nucleus scattering amplitude is given by $\mathcal{N}_A(x, \boldsymbol{r}, \boldsymbol{b}_A) = \{1 - [1 - \tfrac{1}{2}\sigma_{dp}(x, \boldsymbol{r}^2) T_A(\boldsymbol{b}_A)]^A\}$, which reduces to an exponentiated form for large A (see, e.g., Refs. [28,38]). One has verified that, for oxygen, the predictions derived using these two approximations are almost identical, differing by a few percent ($\leqslant 5\%$).
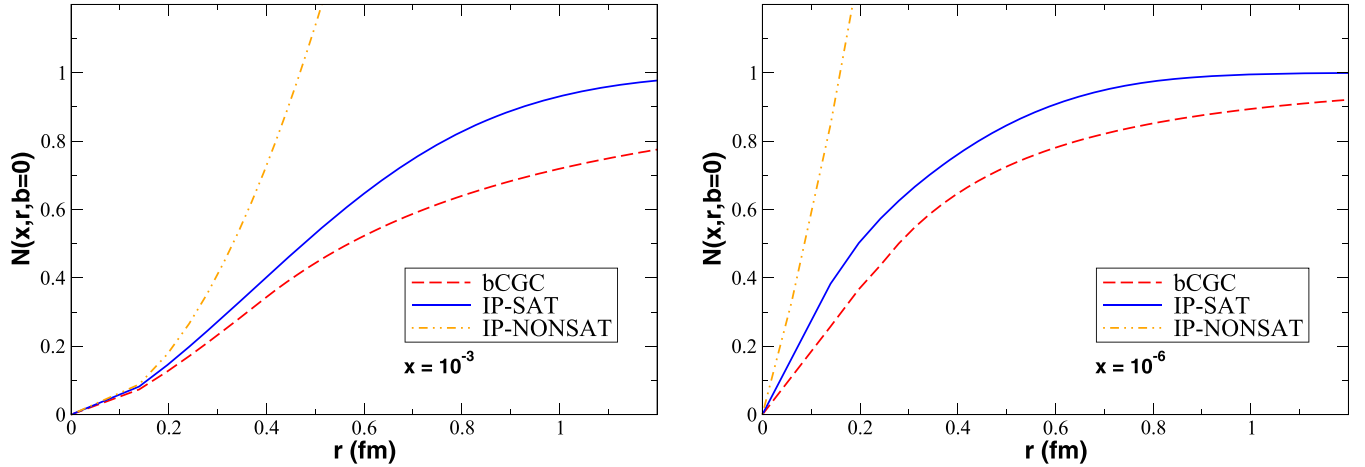
FIG. 2. Dipole-proton scattering amplitude as a function of the dipole size r for two distinct values of x and central collisions ($b_p = 0$).

that $\mathcal{N}^p \propto r^2\, xg(x, 4/r^2)$. On the other hand, for large dipole sizes, the IP-SAT amplitude has an asymptotic value larger than the bCGC one. For $x = 10^{-6}$ we have that the onset of the saturation occurs at smaller values of r. The main difference between the bCGC and IP-SAT models is associated with the behavior predicted for the transition between the linear (small-r) and nonlinear (large-r) regimes of the QCD dynamics. Moreover, it is important to emphasize that the nonlinear effects strongly modify the behavior of $\mathcal{N}_p$ at large r in comparison to the linear prediction.

In order to analyze the dependence of our predictions on the model assumed for the overlap function $(\Psi^{V*}\Psi)_T$, we present in Fig. 3 the behavior of the quantity

$$W(\mathbf{r}) = 2\pi r \int_0^1 dz [\Psi^{V*}(\mathbf{r}, z)\Psi(\mathbf{r}, z)]_T, \quad (6)$$

as a function of $\mathbf{r}$ for different vector mesons, considering the BG and GLC models for the vector meson function. We find that both models predict a peak in the function $W(r)$. The position of the peak is almost model independent, with
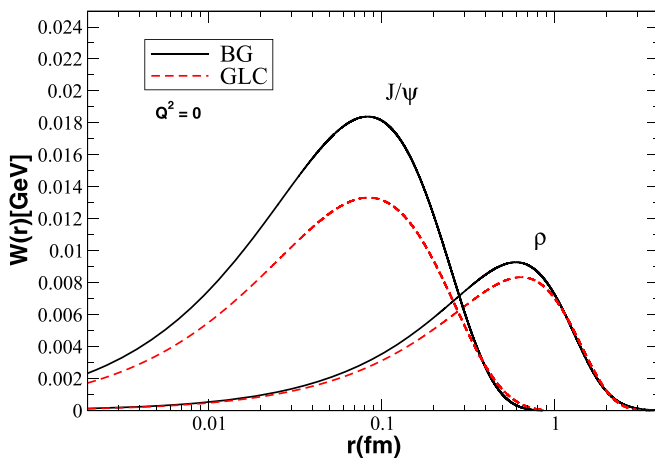

FIG. 3. Dependence on the dipole size r of the function $W(\mathbf{r})$ for the ρ and J/Ψ mesons considering the boosted-Gaussian (BG) and Gaus-LC (GLC) models for the vector meson wave functions.

the normalization of the GLC model being smaller than that of the BG model. Moreover, the peak occurs at larger values of $\mathbf{r}$ for the ρ meson, while for the J/Ψ photoproduction it occurs for smaller dipoles. Such a result indicates that for the J/Ψ photoproduction the main contribution for the amplitude comes from dipoles with $r \approx 0.09$ fm, while for the ρ case one has $r \approx 0.7$ fm. Therefore, studying ρ and J/Ψ photoproduction we are mapping different configurations of the dipole size, which probe different regimes of the QCD dynamics, as demonstrated in Fig. 2. It is important to clarify that the predictions for the ρ photoproduction derived using the dipole formalism can be strongly affected by nonperturbative corrections not taken into account in our analysis. From Fig. 3 one has that the contribution of dipoles with size larger than 0.7 fm is $\approx 40\%$ for the ρ case. Therefore, the description of the ρ photoproduction using a perturbative approach is not fully justified. However, as the nonlinear effects imply that the contribution of small-size dipoles increases for smaller values of x, one can expect that in the asymptotic regime $W \rightarrow \infty$ ($x \rightarrow 0$) such a process could be estimated perturbatively. An open question is if the magnitude of Q_s for the energies probed by the current colliders already is large enough to justify the treatment using the dipole approach. As pointed out in the Introduction, the dipole predictions provide a reasonable description of the existing HERA and ALICE data. However, we believe that a larger amount of data is needed before establishing that such an agreement is not accidental. Having it in mind, the comparison of the dipole predictions presented in this paper with the data that can be obtained in future pO collisions will be useful to improve our understanding of the ρ photoproduction.

Let us now discuss the exclusive ρ and J/Ψ photoproduction in pO collisions. For a fixed rapidity, the photon fluxes for the proton and oxygen will be determined by ω_L and ω_R, respectively, i.e., will probe the photon fluxes in different energy ranges. Moreover, the distribution will be given by the cross sections for γp and γO interactions. In γp interactions the photon comes from the oxygen, with the photon flux being proportional to Z^2 ($Z = 8$), and the photoproduction cross section depends on the square of $\mathcal{N}_p$. In γO interactions the photon comes from the proton, and the photoproduction
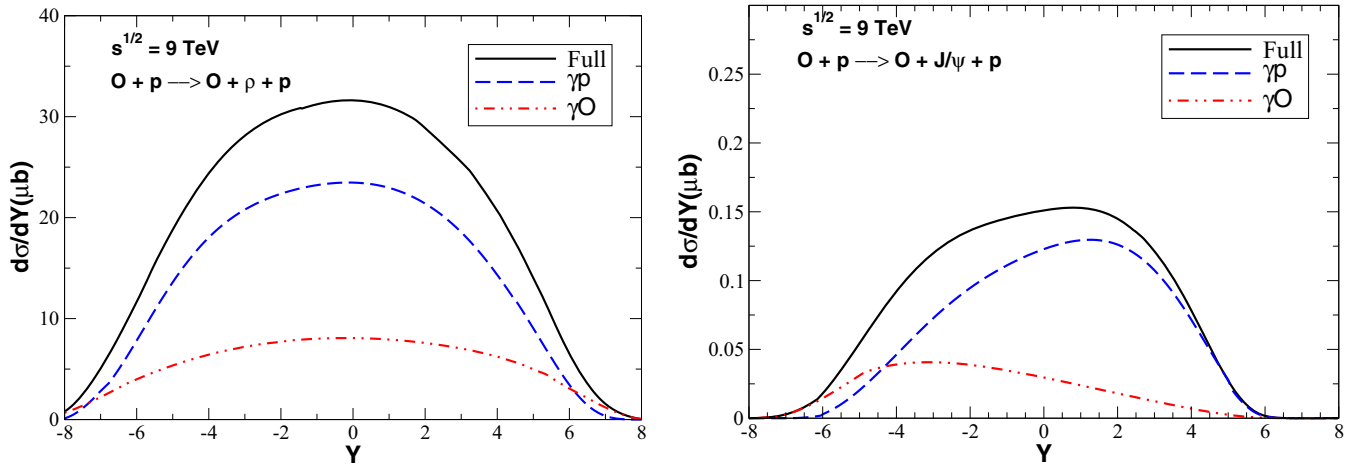
FIG. 4. Rapidity distributions for the exclusive ρ (left panel) and J/Ψ (right panel) photoproduction in ultraperipheral pO collisions, obtained using the boosted-Gauss model for the vector meson wave functions and assuming the bCGC model as input in the calculations of the scattering amplitudes $\mathcal{N}_p$ and $\mathcal{N}_O$. The contributions associated with γp and γO interactions are presented separately as well as the sum of the contributions, denoted as Full in the figure.

cross section is determined by the square of $\mathcal{N}_O$. As a consequence, asymmetric rapidity distributions are expected in pO collisions. Moreover, one has that the shape of the distribution will be dependent on the model assumed for the dipole-target scattering amplitude and the vector meson that is produced. Such dependencies are expected since the distribution for a given rapidity Y is determined by the product between the photon flux for the photon energy $\omega = M_V/2 \exp(+Y)$ and the photon-target cross section for the corresponding photon-target center-of-mass energy $W = \sqrt{2\omega\sqrt{s}}$. As the photon energy is dependent on the meson mass and the increasing of the cross section with the energy is distinct for the different models assumed for the overlap function and dipole-target scattering amplitude considered in our analysis, we expect that the shape of the distribution will be different for ρ and J/Ψ photoproduction. Such expectations are confirmed by the results shown in Figs. 4 and 5 (upper panels).

In Fig. 4 the predictions for the rapidity distributions for the exclusive ρ (left panel) and J/Ψ (right panel) photoproduction in ultraperipheral pO collisions, derived in the center-of-mass frame and obtained by integrating over t the Eq. (1). For this first analysis, we use the BG model for the vector meson wave functions and assume the bCGC model as input in the calculations of the scattering amplitudes $\mathcal{N}_p$ and $\mathcal{N}_O$. The O beam is assumed to be moving from negative to positive rapidities and we present separately the contributions associated with γp and γO interactions as well as the sum of the contributions, denoted as Full in the Fig. 4. One has that the contribution of γO interactions is non-negligible and can dominate for some values of rapidity, in contrast with the results obtained for pPb collisions, where the γPb contribution can be disregarded. Such a difference arises due to two aspects: (a) the Z^2 enhancement in the photon flux for the oxygen is not a large number, and (b) the maximum energy of the emitted photons by a particle is inversely proportional to its radius, which implies that larger photon-ion center-of-mass energies are reached in ultraperipheral pO collisions in

comparison to pPb collisions, which is important when the cross sections increase with the energy as in the process under analysis.

The dependence of our predictions for the rapidity distributions on the models assumed for the overlap function and for the description of the dipole-target cross sections are presented in Fig. 5 considering the exclusive ρ (left panels) and J/Ψ (right panels) photoproduction in ultraperipheral pO (upper panels) and OO (lower panels) collisions. One has that the GLC model for the overlap function diminishes the normalization of the predictions, with a small impact on the shape of the distributions. In contrast, our results for pO collisions (upper panels) indicate that the rapidity distribution is sensitive to the description of the QCD dynamics. In particular, the asymmetry with relation to $Y = 0$ for the ρ photoproduction is different for the bCGC and IP-SAT models due to the distinct behaviors for the transition between the linear (small-r) and nonlinear (large-r) regimes (see Fig. 2). In contrast, for the J/Ψ photoproduction, which is dominated by dipoles of small size, one has that both models predict that the maximum of the distribution occurs for positive rapidities. Such results indicate that the analyses of both final states can be useful to discriminate between these approaches for the QCD dynamics. For OO collisions (lower panels), we have that the main difference between the predictions arises from the model assumed for the overlap function, which is expected due to the fact that the change of bCGC for IP-SAT only affects the argument of the exponential in the Glauber-Mueller model for the dipole-nucleus scattering amplitude [see Eq. (4)]. The corresponding predictions for the total cross sections are presented in Tables I and II for the rapidity ranges covered by the ALICE and LHCb detectors, respectively. For the LHCb detector, which probes an asymmetric range of rapidities, we present our predictions for pO and Op collisions. We predict values of $\mathcal{O}$ (mb) [$\mathcal{O}$ (μb)] for the ρ [J/Ψ] photoproduction in OO collisions, with the predictions for pO collisions being smaller by approximately 1 order of magnitude. Considering
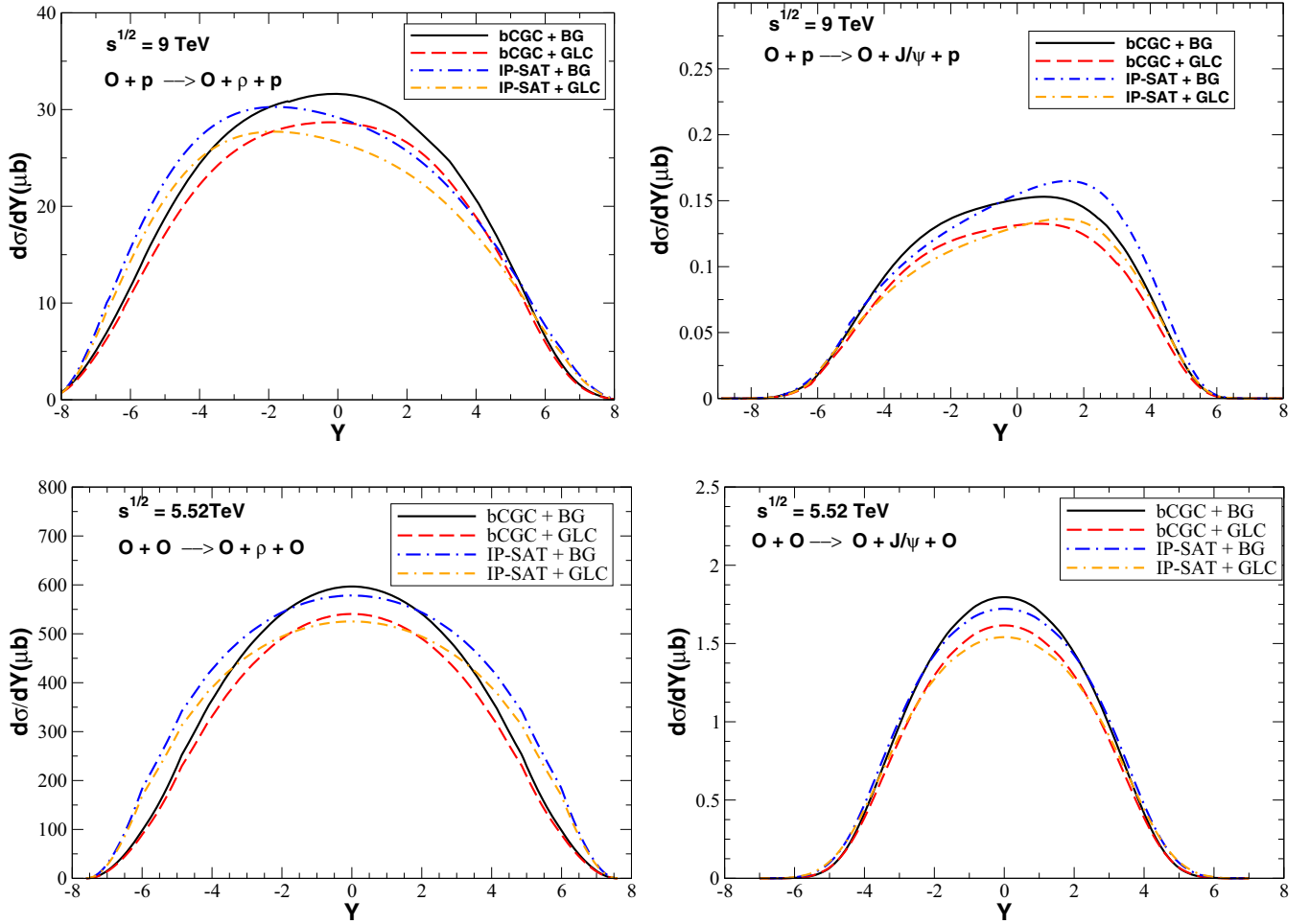
FIG. 5. Rapidity distributions for the exclusive ρ (left panels) and J/Ψ (right panels) photoproduction in ultraperipheral pO (upper panels) and OO (lower panels) collisions considering different models for the overlap function and for the description of the dipole-target cross sections.

TABLE I. Total cross sections (in μb) for the exclusive ρ and J/ψ photoproduction in ultraperipheral pO ($\sqrt{s} = 9$ TeV) and OO ($\sqrt{s} = 5.52$ TeV) collisions at the LHC. Predictions for the rapidity range covered by the ALICE detector derived considering different models for the description of the dipole-hadron interaction and for the modeling of the overlap function.

ALICE ($-2.5 \leqslant Y \leqslant 2.5$)	ρ in OO collisions	ρ in pO collisions	J/ψ in OO collisions	J/ψ in pO collisions
bCGC + BG	2837.62	152.70	8.06	0.73
bCGC + GLC	2571.39	139.24	7.25	0.63
IP-SAT + BG	2800.92	142.77	7.85	0.75
IP-SAT + GLC	2545.44	130.45	7.01	0.63

TABLE II. Total cross sections (in μb) for the exclusive ρ and J/ψ photoproduction in ultraperipheral pO ($\sqrt{s} = 9$ TeV) and OO ($\sqrt{s} = 5.52$ TeV) collisions at the LHC. Predictions for the rapidity range covered by the LHCb detector derived considering different models for the description of the dipole-hadron interaction and for the modeling of the overlap function.

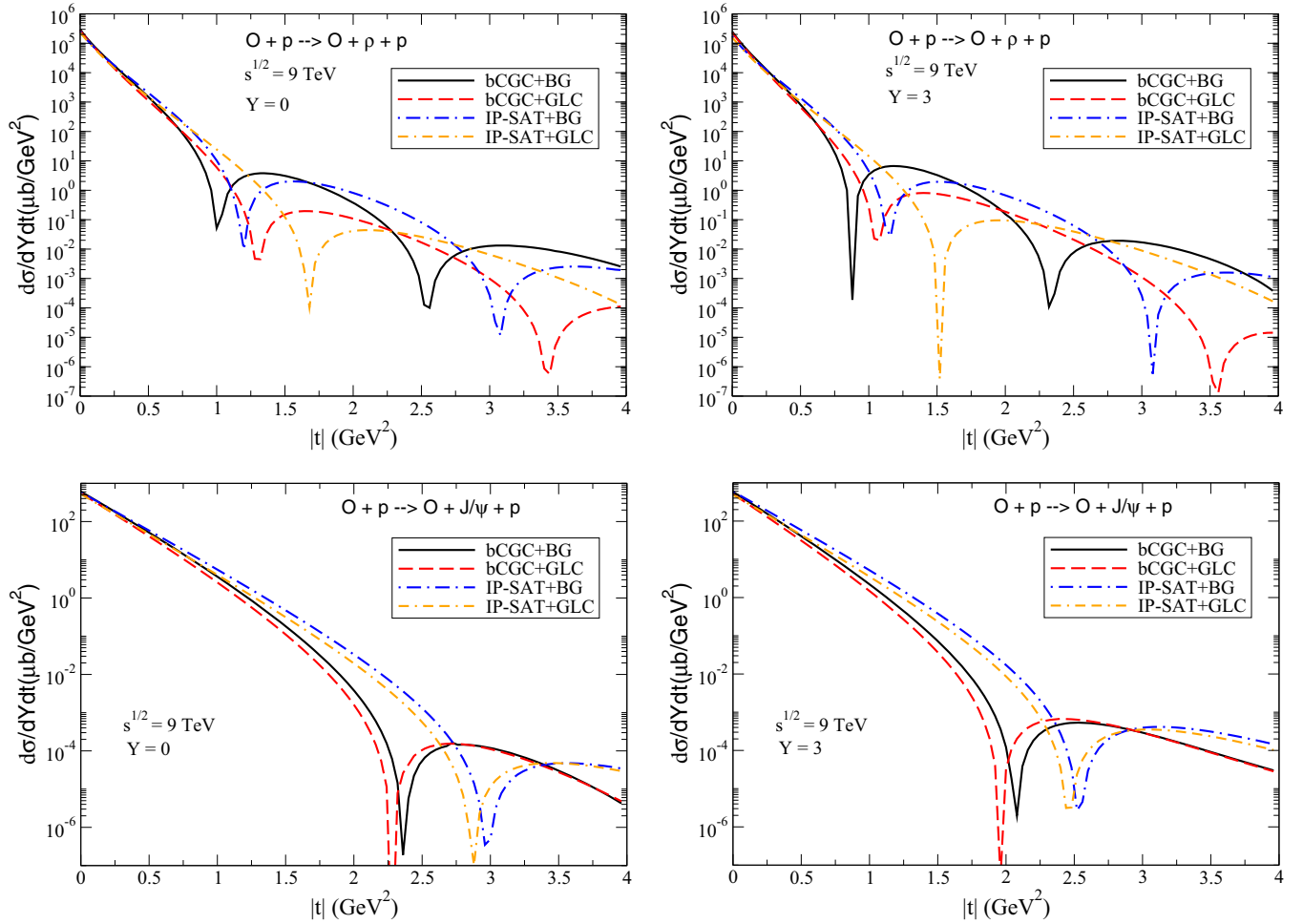| LHCb ($2.0 \leqslant Y \leqslant 4.5$)	ρ in OO collisions	ρ in pO (Op) collisions	J/ψ in OO collisions	J/ψ in pO (Op) collisions
bCGC + BG	1092.85	60.20 (67.15)	2.06	0.27 (0.28)
bCGC + GLC	991.52	55.33 (61.31)	1.88	0.23 (0.24)
IP-SAT + BG	1189.18	53.87 (71.54)	2.15	0.31 (0.26)
IP-SAT + GLC	1083.71	49.10 (65.61)	1.95	0.25 (0.23)

FIG. 6. Predictions for the t distribution of the exclusive ρ (upper panels) and J/Ψ (lower panels) photoproduction in ultraperipheral pO collisions for two values of the meson rapidity: $Y = 0$ (left panels) and $Y = 3$ (right panels).

the large values of luminosity expected in the case of collisions with oxygen ions, we can expect a large number of events, which makes the experimental analysis, in principle, feasible.

The predictions for the t distribution of the exclusive vector meson photoproduction in ultraperipheral pO collisions, derived considering distinct models for $\mathcal{N}_p$ and for the overlap function, are presented in Fig. 6 considering two distinct values for the meson rapidity Y and that γp interactions are dominant. The results indicate that the distribution is strongly dependent on the model considered for the dipole-proton scattering amplitude and for the overlap function. One has that both the bCGC and IP-SAT models predict dips at large values of $|t|$, with its positions being dependent on the model considered.[3] One has that the first dip occurs for smaller

values of $|t|$ when the rapidity is increased and for the ρ photoproduction. We also have that for the ρ photoproduction, the position of the first dip is strongly dependent on the model assumed for the overlap function. Such is not the case for the J/Ψ photoproduction (lower panels), which implies that the analysis of this final state can be useful to constrain the modeling of the QCD dynamics. As already pointed out in the case of the rapidity distribution, these results also indicate that the best way to improve our understanding about the QCD dynamics and vector meson photoproduction is the simultaneous analysis of both final states. The corresponding results for OO collisions are presented in Fig. 7. As in the pO case, the position of the first dip occurs for smaller values of $|t|$ for larger rapidities and in the case of the ρ photoproduction. Moreover, one has that the positions of the first two dips are similar and become gradually distinct at larger values of $|t|$.

---

[3] It is important to emphasize that similar conclusions are also derived if we consider the exclusive vector meson photoproduction at HERA. However, due to experimental restrictions, the H1 and ZEUS Collaborations were not able to measure the coherent ρ and J/Ψ photoproduction at large $|t|$, where the dips are predicted to occur.

As demonstrated, e.g., in Refs. [30,32], the current HERA data for low values of $|t|$ are quite well described by the bCGC and IP-SAT models.
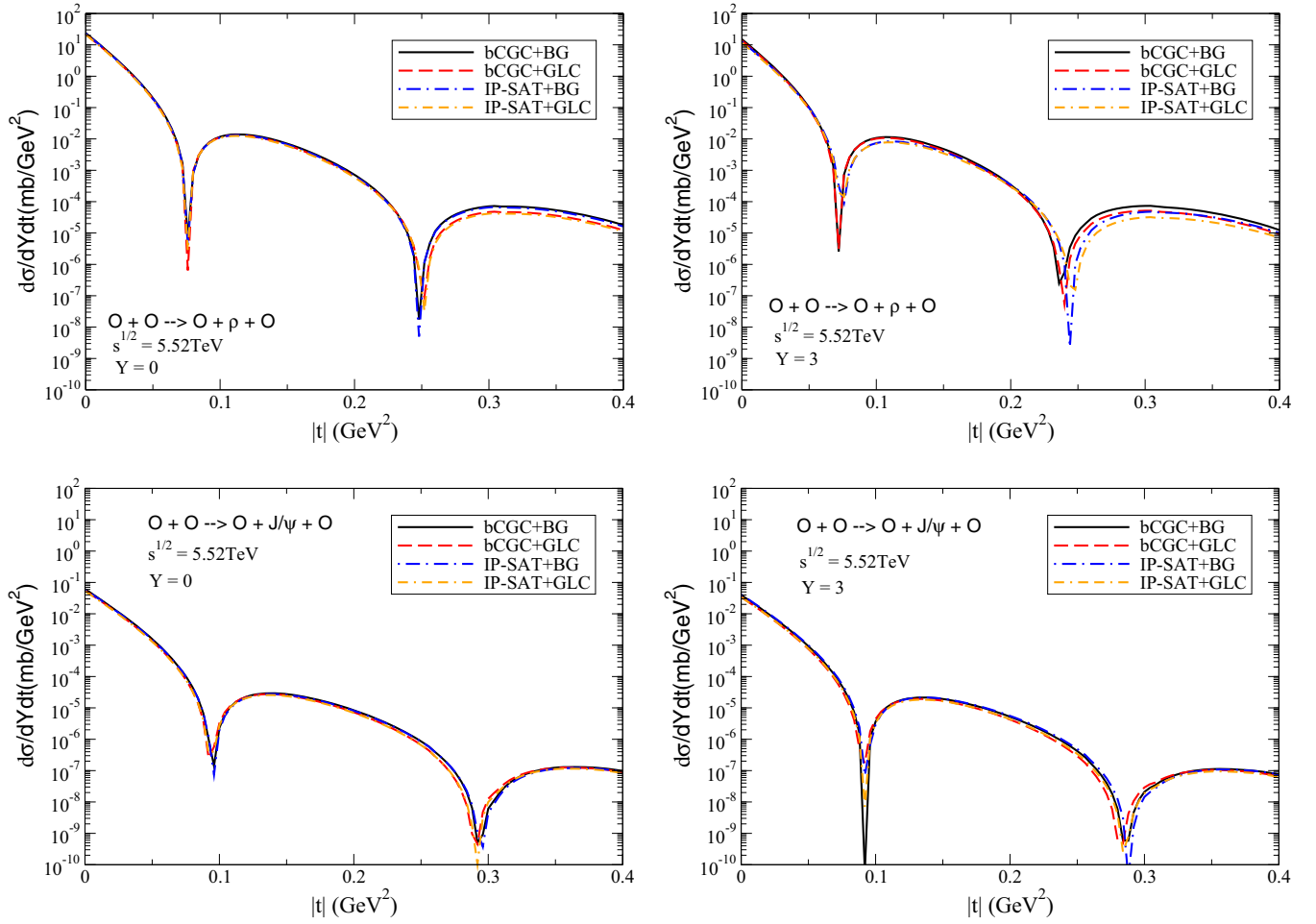
FIG. 7. Predictions for the t distribution of the exclusive ρ (upper panels) and J/Ψ (lower panels) photoproduction in ultraperipheral OO collisions for two values of the meson rapidity: $Y = 0$ (left panels) and $Y = 3$ (right panels).

In other words, in order to discriminate the treatment of the QCD dynamics at the proton level, we should probe values of $|t| \gtrsim 0.2$ GeV^2.

A final comment about the feasibility of measurements of the ρ and J/Ψ photoproduction in pO and OO collisions is in order. A current shortcoming to estimate the number of events is associated with the fact that the value of the average luminosity and the number of days available for data acquisition during Run 3 are still the subject of intense debate. It was discussed in Ref. [2] that values of the order of $7 \times 10^5 \ \mu\text{b}^{-1}$ could be reached in future runs. Assuming this value and considering our predictions for the total cross sections presented in Tables I and II, we predict that the number of ρ (J/Ψ) events at ALICE considering OO collisions will be larger than 17×10^7 (49×10^5). For pO collisions, the predictions are 1 order of magnitude smaller. As the transverse momentum distributions decrease for large t (see, e.g., Fig. 6), the number of events will be strongly reduced if a cut on the minimum value of t is assumed. As a consequence, a future analysis of the t distribution in pO collisions will be a challenge for the experimentalists considering the expected luminosity.

IV. SUMMARY

The analysis of the exclusive vector meson photoproduction in hadronic colliders is considered one of the most promising ways to constrain the QCD dynamics at high energies. In recent years, several studies were performed considering the production of heavy and light vector mesons in pp, pPb, and PbPb collisions at different center-of-mass energies and/or distinct ranges of rapidity. Study of these different configurations is fundamental to constrain the description of the underlying dynamics since the impact of the nonlinear effects are determined by the magnitude of the saturation scale, which is predicted to be energy dependent and atomic number dependent and is expected to be larger in processes dominated by larger dipole sizes. Such aspects strongly motivate a future experimental analysis of the exclusive ρ and J/Ψ photoproduction in ultraperipheral pO and OO collisions, since these collisions will probe a new kinematical range, complementary to that mapped by previous studies. In particular, they will allow us to improve our understanding about the energy and nuclear dependencies of the saturation scale, as well as the description of the linear and nonlinear regimes,

which are expected to determine the behavior of the cross sections for the J/Ψ and ρ photoproduction, respectively. In this paper we have estimated the rapidity and transverse momentum distributions for pO collisions at $\sqrt{s} = 9$ TeV and OO collisions at $\sqrt{s} = 5.52$ TeV, which can be analyzed in forthcoming years. Moreover, we have presented our predictions for the total cross sections considering the rapidity ranges covered by the ALICE and LHCb detectors. Different approaches for the dipole-target scattering amplitude and for the treatment of the overlap function were considered, which allowed us to estimate the current theoretical uncertainty on our predictions. Our results indicate that a future experimental analysis is, in principle, feasible. Considering

the results presented in this paper and those in Refs. [9,10], we strongly encourage the investigation of the ρ and J/Ψ photoproduction in pO and pPb collisions in order to discriminate the distinct approaches for the QCD dynamics at high energies.

[1] M. Begel, S. Hoeche, M. Schmitt, H. W. Lin, P. M. Nadolsky, C. Royon, Y. J. Lee, S. Mukherjee, J. Campbell, F. G. Celiberto *et al.*, arXiv:2209.14872.

[2] Z. Citron, A. Dainese, J. F. Grosse-Oetringhaus, J. M. Jowett, Y. J. Lee, U. A. Wiedemann, M. Winn, A. Andronic, F. Bellini, E. Bruna *et al.*, CERN Yellow Rep.: Monogr. **7**, 1159 (2019).

[3] J. Brewer, A. Mazeliauskas, and W. van der Schee, arXiv:2103.01939.

[4] M. D. Sievert and J. Noronha-Hostler, Phys. Rev. C **100**, 024904 (2019).

[5] H. P. Dembinski, R. Ulrich, and T. Pierog, PoS **ICRC2019**, 235 (2020).

[6] P. Paakkinen, Phys. Rev. D **105**, L031504 (2022).

[7] C. A. Bertulani and G. Baur, Phys. Rep. **163**, 299 (1988); F. Krauss, M. Greiner, and G. Soff, Prog. Part. Nucl. Phys. **39**, 503 (1997); C. A. Bertulani, S. R. Klein, and J. Nystrand, Annu. Rev. Nucl. Part. Sci. **55**, 271 (2005); V. P. Goncalves and M. V. T. Machado, J. Phys. G: Nucl. Part. Phys. **32**, 295 (2006); A. J. Baltz *et al.*, Phys. Rep. **458**, 1 (2008); J. G. Contreras and J. D. Tapia Takaki, Int. J. Mod. Phys. A **30**, 1542012 (2015); K. Akiba *et al.*, [LHC Forward Physics Working Group], J. Phys. G: Nucl. Part. Phys. **43**, 110201 (2016); S. R. Klein and H. Mantysaari, Nat. Rev. Phys. **1**, 662 (2019); S. Klein and P. Steinberg, Annu. Rev. Nucl. Part. Sci. **70**, 323 (2020).

[8] V. P. Gonçalves, M. V. T. Machado, B. D. Moreira, F. S. Navarra, and G. S. dos Santos, Phys. Rev. D **96**, 094027 (2017).

[9] V. P. Gonçalves, F. S. Navarra, and D. Spiering, Phys. Lett. B **768**, 299 (2017).

[10] V. P. Gonçalves, F. S. Navarra, and D. Spiering, Phys. Lett. B **791**, 299 (2019).

[11] F. Gelis, E. Iancu, J. Jalilian-Marian, and R. Venugopalan, Annu. Rev. Nucl. Part. Sci. **60**, 463 (2010); H. Weigert, Prog. Part. Nucl. Phys. **55**, 461 (2005); J. Jalilian-Marian and Y. V. Kovchegov, *ibid.* **56**, 104 (2006); A. Morreale and F. Salazar, Universe **7**, 312 (2021).

[12] V. P. Gonçalves and M. V. T. Machado, Eur. Phys. J. C **40**, 519 (2005).

[13] V. P. Gonçalves, M. V. T. Machado, and A. R. Meneses, Eur. Phys. J. C **68**, 133 (2010).

[14] G. Sampaio dos Santos and M. V. T. Machado, Phys. Rev. C **91**, 025203 (2015).

[15] M. Ahmady, R. Sandapen, and N. Sharma, Phys. Rev. D **94**, 074018 (2016).

[16] Y. P. Xie and X. Chen, Eur. Phys. J. C **76**, 316 (2016).

[17] S. R. Klein and J. Nystrand, Phys. Rev. C **60**, 014903 (1999).

[18] V. P. Gonçalves and C. A. Bertulani, Phys. Rev. C **65**, 054905 (2002).

[19] L. Frankfurt, M. Strikman, and M. Zhalov, Phys. Lett. B **540**, 220 (2002).

[20] S. Klein, D. Tapia Takaki, J. Adam, C. Aidala, A. Angerami, B. Audurier, C. Bertulani, C. Bierlich, B. Blok, J. D. Brandenburg *et al.*, arXiv:2009.03838.

[21] H. Mäntysaari, F. Salazar, and B. Schenke, Phys. Rev. D **106**, 074019 (2022).

[22] M. Drees and D. Zeppenfeld, Phys. Rev. D **39**, 2536 (1989).

[23] Y. Hatta, B. W. Xiao, and F. Yuan, Phys. Rev. D **95**, 114026 (2017).

[24] H. Mäntysaari, K. Roy, F. Salazar, and B. Schenke, Phys. Rev. D **103**, 094026 (2021).

[25] H. G. Dosch, T. Gousset, G. Kulzinger, and H. J. Pirner, Phys. Rev. D **55**, 2602 (1997).

[26] J. Nemchik, N. N. Nikolaev, E. Predazzi, and B. G. Zakharov, Z. Phys. C **75**, 71 (1997).

[27] J. R. Forshaw, R. Sandapen, and G. Shaw, Phys. Rev. D **69**, 094013 (2004).

[28] H. Kowalski and D. Teaney, Phys. Rev. D **68**, 114005 (2003).

[29] H. Kowalski, L. Motyka, and G. Watt, Phys. Rev. D **74**, 074016 (2006).

[30] A. H. Rezaeian, M. Siddikov, M. Van de Klundert, and R. Venugopalan, Phys. Rev. D **87**, 034002 (2013).

[31] J. Jalilian-Marian, A. Kovner, L. McLerran, and H. Weigert, Phys. Rev. D **55**, 5414 (1997); J. Jalilian-Marian, A. Kovner, A. Leonidov, and H. Weigert, *ibid.* **59**, 014014 (1998); **59**, 034007 (1999); A. Kovner, J. G. Milhano, and H. Weigert, Nucl. Phys. A **703**, 823 (2002); Phys. Rev. D **62**, 114005 (2000); E. Iancu, A. Leonidov, and L. McLerran, Nucl. Phys. A **692**, 583 (2001); E. Ferreiro, E. Iancu, A. Leonidov, and L. McLerran, *ibid.* **703**, 489 (2002).

[32] A. H. Rezaeian and I. Schmidt, Phys. Rev. D **88**, 074016 (2013).

[33] Yu. Dokshitzer, Sov. Phys. JETP **46**, 641 (1977); V. N. Gribov and L. N. Lipatov, Sov. J. Nucl. Phys. **15**, 438 (1972); G. Altarelli and G. Parisi, Nucl. Phys. B **126**, 298 (1977).

[34] R. J. Glauber, in *Lectures in Theoretical Physics*, edited by W. E. Brittin and L. G. Duham (Interscience, New York, 1959), Vol. 1.

[35] V. N. Gribov, Sov. Phys. JETP **29**, 483 (1969); **30**, 709 (1970).

[36] A. H. Mueller, Nucl. Phys. B **335**, 115 (1990).

[37] N. Armesto, Eur. Phys. J. C **26**, 35 (2002).

[38] H. Kowalski, T. Lappi, C. Marquet, and R. Venugopalan, Phys. Rev. C **78**, 045201 (2008).

[39] H. Mäntysaari, Rep. Prog. Phys. **83**, 082201 (2020).

[40] H. Mäntysaari and B. Schenke, Phys. Rev. Lett. **117**, 052301 (2016).

[41] H. Mäntysaari and B. Schenke, Phys. Lett. B **772**, 832 (2017).

[42] J. Cepila, J. G. Contreras, and M. Krelina, Phys. Rev. C **97**, 024901 (2018).

[43] M. Krelina, V. P. Goncalves, and J. Cepila, Nucl. Phys. A **989**, 187 (2019).

[44] R. Boussarie, A. V. Grabovsky, D. Y. Ivanov, L. Szymanowski, and S. Wallon, Phys. Rev. Lett. **119**, 072002 (2017).

[45] T. Lappi, H. Mäntysaari, and J. Penttala, Phys. Rev. D **102**, 054020 (2020).

[46] G. Beuf, H. Hänninen, T. Lappi, and H. Mäntysaari, Phys. Rev. D **102**, 074028 (2020).

[47] H. Mäntysaari and J. Penttala, Phys. Lett. B **823**, 136723 (2021).

[48] H. Mäntysaari and J. Penttala, Phys. Rev. D **105**, 114038 (2022).

[49] H. Mäntysaari and J. Penttala, J. High Energy Phys. 08 (2022) 247.